SURFACE MICROTHERMOCOUPLE CHARACTERIZATION AND MATHEMATICAL MODELING IN RADIATIVE CONDITIONS

Y. Doghmane*, F. Lanzetta*, E. Gavignet*, R. Glises*, Y. Bailly* and P. Blind**

* FEMTO-ST Institut – UMR 6174
CNRS/Franche-Comte University/ENSMM/UTBM
Energy Department
2 avenue Jean Moulin 90000 Belfort France
email: francois.lanzetta@univ-fcomte.fr

** Institut Pierre Vernier
Technopôle Temis
24 rue Alain Savary 25000 Besançon France

Résumé

Ce travail porte sur la modélisation et la caractérisation dynamique en mode radiatif d'un microthermocouple de surface destiné à la mesure de température instationnaire. Le microthermocouple est de type K (Chromel /Alumel). La jonction chaude est réalisée à partir d'une couche de tungstène déposée sur un substrat de céramique par une technique de PVD (Physical Vapor Deposition). La caractérisation dynamique est obtenue par la détermination de la réponse impulsionnelle en focalisant sur la jonction chaude un pulse laser de quelques nanosecondes. Les essais numériques et expérimentaux sont réalisés sous faible pression (960 Pa) et à pression atmosphérique (10^5 Pa), les temps de montée obtenus sont de l'ordre de 20 µs à faible pression et 25 µs à pression atmosphérique.

Abstract

This paper presents the dynamic characterization and the mathematical modeling in radiative conditions of a thin film thermocouple for non stationary measurements. This temperature sensor is a K type (Chromel/Alumel) wire microthermocouple which hot junction is obtained from a tungsten layer deposition by PVD process (Physical Vapor Deposition). The aim of this work is to develop a mathematical modeling of dynamic characterization with a radiation source from a laser focused onto the thermocouple's hot junction. Control theory states that the dynamic performance of a sensor can be assessed by measuring its unit-impulse response function. To test the thermal sensor a delta function is approached by a laser pulse of a few nanoseconds duration. Modeling and experiments are realized at low pressure (960 Pa) and atmospheric pressure (10^5 Pa), the rise times are approximately 20 µs at low pressure and 25 µs at atmospheric pressure.

1. Introduction

Thermoelectric thin films are used in various types of applications like thermocouples, flow sensors or heat flux sensors [1-5]. In many cases, the measurements involve sensors with low thermal inertia and fast response time in order to determine the heat transfer rates between the fluid and the wall. When a thermocouple is submitted to a rapid temperature change, it will take some time to respond. If the sensor response time is slow in comparison with the rate of change of the measured temperature the thermocouple will not be able to faithfully represent the dynamic response of the temperature fluctuations. The problem is to measure the true temperature of the fluid because a thermocouple gives its own temperature only. The temperature differences between the fluid and the sensor are also influenced by thermal transport processes taking place between the fluid to be measured, the temperature sensor, the environment and the location of the thermocouple. Consequently the measured temperature values must be corrected. Whereas in steady conditions only the contributions of the conductive, convective and radiative heat exchanges with the external medium occur. Unsteady behaviour introduces another parameter which becomes predominant: the junction thermal lag which is strongly related to its heat capacity and thermal conductivity. The corrections generally decrease with the thermocouple diameters, and both temporal and spatial resolutions are improved. However, while spatial resolution is fairly directly connected with the thermocouple dimensions, temporal resolution does not only depend on the dimensions and the thermocouple physical characteristics but also on the complex heat balance of the whole thermocouple.

This work deals with the realization of a thin film thermocouple and its radiative characterization. A mathematical modeling and an experimental test bench are presented in order to estimate the unsteady behaviour of the sensor. The thermocouple consists of two wires thermocouples with a metallic layer of tungsten for the junction. Its thickness is smaller than a classical junction obtained by capacitive discharge which contributes to a better time behaviour.

2. Mathematical modeling

The simulations of the thermal sensor are performed using the multiphysics simulation software COMSOL (Fig. 1). Two configurations of modeling are considered. The first one concerns the chamber at a pressure of 960 Pa at 20°C. In these experimental conditions the sensor

exchanges heat with the surroundings by radiation only. The second one is performed with an atmospheric pressure (10^5 Pa) in the chamber and heat transfers concern radiation and natural convection with surroundings. The ambient temperature is set to 20°C and the external surfaces of the sensor are considered as blackbodies. The upper surface of the sensor is subjected to a laser pulse (inhomogeneous Neumann boundary conditions) with duration of 15 ns corresponding to the experimental conditions.

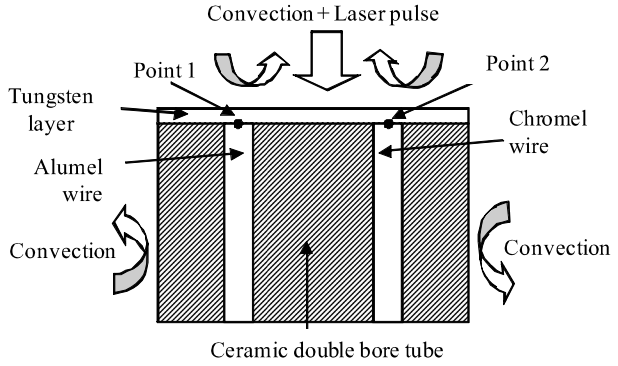

Fig 1– Schematic diagram of the sensor

The view factor between the internal surfaces (blackbodies) of the enclosure and the sensor (blackbody) is automatically generated by the software. Heat transfer between the sensor and the parietal interfaces are taken into account with the boundary conditions of the software.

2.1 Heat transfer by radiation between two surfaces *i* and *j*

The net radiation heat flux $\varphi_{i,j}$ between two surfaces i and j is :

$$\varphi_{i,j} = \varepsilon_i \varepsilon_j S_i S_j \sigma F_{i,j} \left(T_i^4 - T_j^4 \right) \quad (1)$$

Where ε_i and ε_j represent the emissivity coefficients of the surfaces S_i and S_j considered as blackbodies, σ the Stefan-Boltzmann (σ = 5.675 10^{-8} W.m^{-2}.K^{-4}), T_i and T_j the temperatures (K) of the surfaces i et j. $F_{i,j}$ is the view factor taken into account in the modeling.

The radiation temperature of the surfaces positioned around the sensor, are called atmospheric temperatures. They are considered at room temperature when the internal fluid chamber is at room temperature. When the internal pressure is zero (low degree of vacuum in the pressure range 10 < P < 1000 Pa), the atmospheric temperature is the room temperature (20 °C).

2.2 Natural convection heat transfer

The natural convection exists between the surfaces of the sensor and the air. It only occurs when the chamber is at atmospheric pressure (about 1 bar) and will be considered negligible to low pressure of 960 Pa. We will assume that the semi-empirical relations in natural convection are valid for short times (of the order of several tens of microseconds).

The average coefficients of heat exchange by convection, denoted $\bar{h}$ (W.m^{-2}.K^{-1}) are determined by the film temperature corresponding to the arithmetic mean of the wall temperature of the sensor and the free stream temperature.

We must determine the values of dimensionless numbers representing physical phenomena in order to establish the kind of convection and heat transfer coefficient. The structure consists of a horizontal cylindrical surface and two flat surfaces (top and bottom). The nondimensional numbers used to determine the Nusselt number for the evaluation of the coefficient of heat transfer by convection are based on a dimensional approach. We do not give here the final expressions selected.

Case of the vertical cylinder

We consider the convection around the probe, taken along the total length immersed in the fluid. We use the expressions of Nusselt number suitable for a vertical flat plate [6]. The relation (2) gives the expression of the Rayleigh number Ra_L for the cylinder height L:

$$Ra_L = \frac{g\beta \left(T_w - T_{amb} \right) L^3}{\nu\, a} = Pr\, Gr_L \quad (2)$$

Where g is the gravity acceleration (g = 9.81 m.s^{-2}), β the coefficient of isothermal compressibility of the air (K^{-1}), T_w and T_{amb} the wall temperature and ambient temperature (K) respectively, L the length of the cylinder (m), ν the cinematic viscosity of the air at ambient temperature (m^2.s^1), a the thermal diffusivity of the air at ambient temperature (m^2.s^{-1}), Pr the Prandtl number and Gr_L Grashof number.

For the experiments the Grashof number is in the range from 10^4 to 10^9. The mean coefficient of convection is function of Reynolds or Rayleigh number (3) [7]:

$$\bar{h} = \frac{\lambda\, Nu_L}{L} = 0{,}59 \frac{k}{L} Ra_L^{1/4} = 5 \text{ W.m}^{-2}\text{.K}^{-1} \quad (3)$$

k is the thermal conductivity of the air at ambient temperature (W.m^{-1}.K^{-1}).

Case of horizontal surfaces

The upper surface of the probe is similar to a horizontal plane of characteristic length equal to the diameter D of the sensor. The Rayleigh number Ra_D (4) determines the expression of the Nusselt number characterizing the intensity Nu_D convective heat transfer [8].

$$Ra_D = \frac{g\beta \left(T_p - T_{amb} \right) D^3}{\nu\, a} = Pr\, Gr_L \quad (4)$$

The Rayleigh number being less than 10^7, the expression of the mean convection coefficient by convection function of the Nusselt number is given by the expression (5):

$$\bar{h} = \frac{\lambda\, Nu_D}{D} = 0{,}54 \frac{\lambda}{D} Ra_D^{1/4} = 16.3 \text{ W.m}^{-2}\text{.K}^{-1} \quad (5)$$

2.3 Results of the modeling

The results are presented at atmospheric pressure and partial vacuum. They correspond to the temporal evolutions of two temperature points positioned at the interface

ceramic/tungsten/ metallic wires (Fig.3). These two points are positioned at the interfaces Alumel-Tungsten (point 1) and Tungsten-Chromel (point 2) respectively. In any case, the temperature of the thermocouple junction, corresponding to the volume temperature between the two points 1 and 2. However, we have presented the results at point 1 and point 2, the reality is between these two developments. As explained in the next paragraph, the intrinsic value of the temperatures obtained should not be the only factor of comparison is highly dependent on uncertainty in the flux density applied. However, the rise times are slightly impacted due to the high slope of the rise in temperature, both experimental and simulated.

Influence of atmospheric pressure

One can easily find a good agreement between the simulated temperatures and the average value of the experimental temperature in the same experimental conditions by applying a flux density of the sensor head of 1.46 10^{10} W.m^{-2}. Indeed, the average value of temperature is between experimental and simulated extreme temperatures. Results are quite satisfactory. The different diffusivity coefficients of the various materials explain the temperature gradients in the probe. Thus, as can be seen, the highest temperatures concern the point 1 because of a thermal diffusivity of the Alumel lower than that of Chromel.

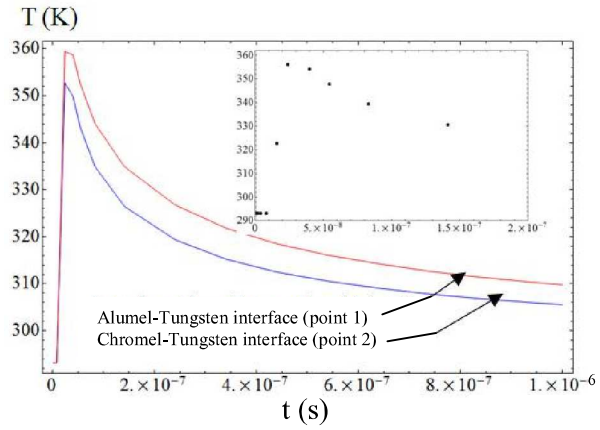

Fig 2 – Simulated temperature profiles at points 1 and 2 and arithmetic mean (Patm = 10^5 Pa)

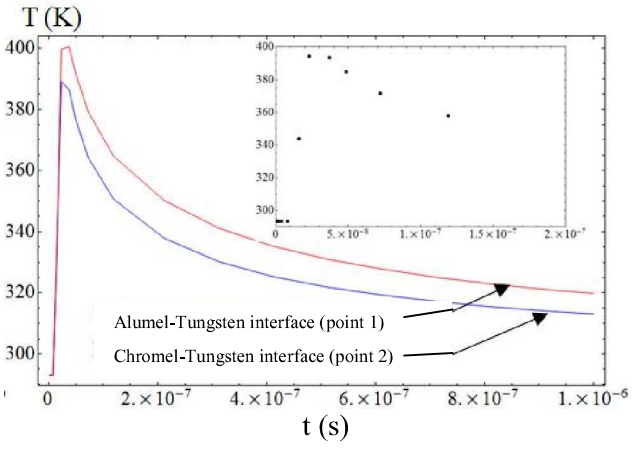

Fig. 3 – Simulated temperature profiles at points 1 and 2 and arithmetic mean (Patm = 960 Pa)

Influence of partial vacuum

A good fit is obtained between simulation and experiment for heat flux density of 2.5 10^{10} W.m^{-2} applied to the sensor head. Figure 3 shows temperature behavior at points 1 and 2 above about 40°C compared to the previous simulation (Fig.2). They are in accordance with the results obtained to those of the corresponding experiments. The relative value of the simulated temperatures at the interfaces 1 and 2 can be explained again in the same way as before by the respective thermal diffusivities of Chromel and Alumel. The experimental rise time (average temperatures at points 1 and 2) presents the same values as atmospheric pressure, ie 25 ns. The simulation shows no significant difference between the two cases, this probably results from the laws of convective heat exchange at the vertical and horizontal surface heat exchanges.

3. Microthermocouple Design

The steps of the microthermocouple realization are represented in Fig. 4 and already described in other works [9].

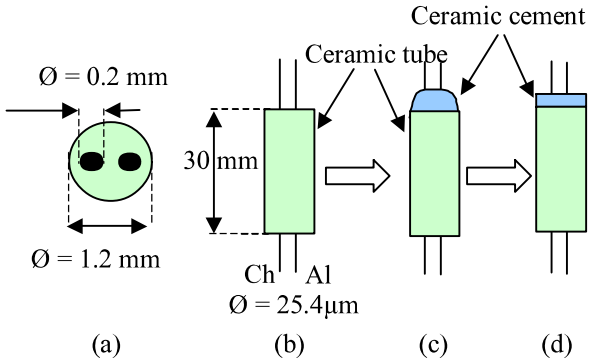

Fig. 4 – Realization of the thermocouple

Two wires (Chromel and Alumel) are inserted in a ceramic double bore tube with 20 mm length and 1.2 mm external diameter to constitute the type K thermocouple (a,b). The wire diameter is fixed at 25.4 µm and this choice corresponds to a standard value used for the laboratory applications. Theses wires are cut with a razor blade and covered by a cement in order to fix the wires and to stuff the empty place in the tube (c). The probe is then heated and smoothed down to obtain a slightly corrugated surface for the junction metallic deposit (d).

In this step, two techniques may be used to realize the junction. The first one consists in connecting several condensers to the thermocouple wires and in welding together with the capacitance discharge. The junction diameter is then similar to the wires diameter [10]. The second technique needs lithographic technology to realize the thermocouple junction. A thin film is deposited on the ceramic cement by Physical Vapour Deposition (PVD) process. This process presents many advantages like the choice of several metals for the film and the control of the deposit thickness. The film thickness may be controlled with different micro fabrication processes and leads to layers with a very fast response time (few nanoseconds for a laser pulse focused on the junction) [11-13] and a high

spatial resolution. Moreover, different materials may be employed in the deposit which gives different thermal sensitivities [14]. The metal deposit is obtained with a 0.8 µm thickness tungsten coat. Tungsten has the highest melting point among metals with temperature values ranging from 3115 to 3160 K. This material has the lowest coefficient of thermal expansion and vapour pressure of all metals. Tungsten hot junction of the thermocouple forms a black surface and presents a good thermal absorptivity. The sensor is represented on Fig. 5 with the ceramic tube and the tungsten layer on its surface.

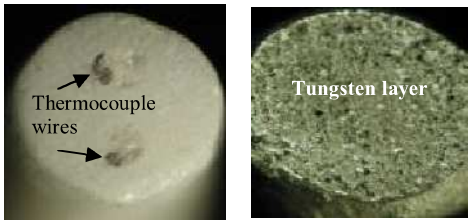

Fig. 5 – Thermocouple design

All thermocouples have to be characterized to determinate the Seebeck coefficient. This static determination is realized with an oven temperature regulated and a standard K type thermocouple is used as reference. Each thermocouple is introduced in this oven and the output signal is measured with a National Instrument data acquisition system (described in §4) and compared to the reference signal for different temperatures varying from 20 °C to 200 °C. The results are not presented in this work but the values of the Seebeck coefficients obtained with this method are equal to 40 µV/°C at 20°C and appropriate to a K type thermocouple. Moreover, the total electrical resistance of the probe (thin film, wires and ceramic substrate) varies from 30 to 50 Ω.

4. Experimental setup for radiative characterization

Figure 6 describes the experimental setup for the radiation test bench. The experimental system consists of a laser system, an optical lens and a data acquisition system. A single laser pulse with duration of 15 ns and a 6.5 mJ at 532 nm energy beam is produced with a YAG laser. The repetition frequency of the pulses can vary from 1 to 15 Hz. The laser beam is focused on the thermocouple junction with the optical lens and a three axis table is used to adjust the thermocouple position. Moreover, the studied thermocouple and a reference thermocouple (type K) are introduced in a vacuum chamber in order to study the pressure effect on the sensor response. Different responses may be obtained for static pressures varying from 900 Pa to 10^5 Pa. The thermocouples are connected directly to a data acquisition system from National Instrument Corporation driven by a software written in LabVIEW© graphic language. The signals are amplified and conditioned by low noise SCXI modules to measure the temperature and to realize the cold junction compensation. They are registered with the data acquisition system operating at the maximum sample rate (200 kHz).

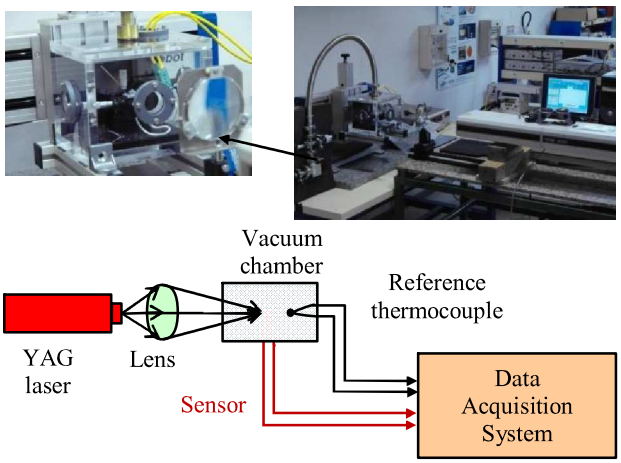

Fig. 6 – Radiative characterization.

This maximum value is necessary to record without errors the sensor response. All wires and connections around the sensor are protected to the temperature fluctuations with ceramic cement. The radiative characterization consists in measuring and recording the junction temperature variations caused by the laser pulse. The main is to determine the time constants as shown in Fig 7. These experiments were completed for a vacuum chamber temperature of 27°C (reference coming from the second thermocouple) and two different pressures: ambient pressure equal to 10^5 Pa (Fig. 7) and 960 Pa (Fig. 8).

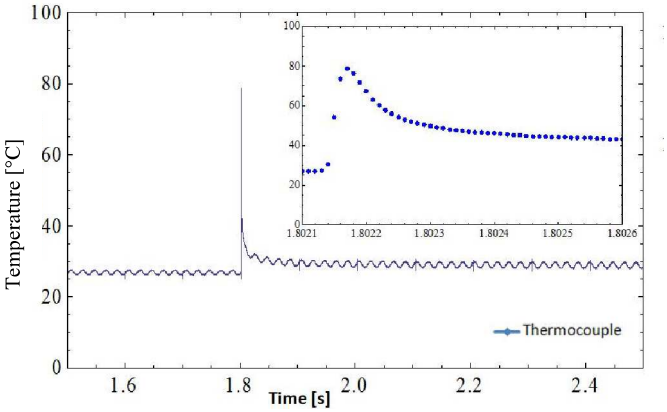

Fig. 7 – Microthermocouple response to a laser pulse ($P=10^5$ Pa)

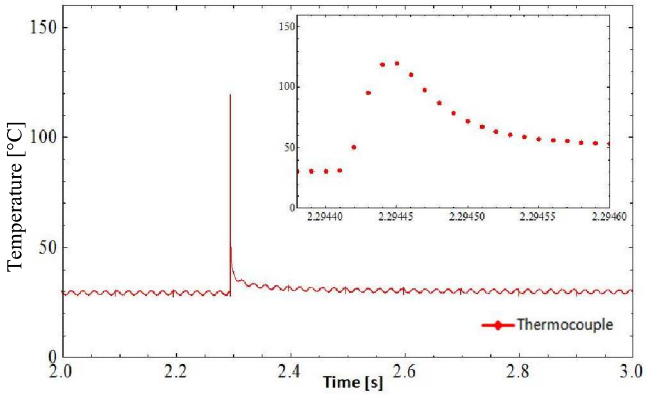

Fig. 8 – Microthermocouple response to a laser pulse (P=960 Pa)

The pulse response shows two characteristic times in the cooling step which means that the system is not a first order. The time constant cannot be obtained by measuring the time that corresponds to 63.2 percent of the final value. In order to avoid the determination of the system order, we have chosen to characterize the time behaviour of the sensor with the determination of the duration to increase the signal response from 10 to 90 percent of the final value. The principle of the rising time determination is represented Fig. 7 and gives a value about 25 µs for ambient pressure. This value corresponds to the response of the probe (tungsten film, ceramic tube and connections) and is different of the layer response which is much smaller. At a pressure of 960 Pa, the rising time is equal to 20 µs which means that the convection contributes to the cooling of the junction under ambient pressure. The rising time also decreases for the increasing of the laser power.

In comparison with the values obtained for different works in radiative mode the results are higher than the general values for thin film thermocouples [13, 15] but it is important to distinguish the thin layer response and the sensor response (our sensor). However, the thin thermocouple performances are better than wires technology thermocouple [9, 10]. These sensors give time constant in radiative mode varying from 70 µs to 180 µs for wires diameters of 0.5 µm and 1.27 µm respectively (S type thermocouples).

5. Conclusion

We characterized the response of the sensors in the presence of gases at different temperatures for pressures fluctuating. We developed a numerical model of thermal behavior validated at different pressures and temperatures. This initial work allowed us to achieve a pressure range between a low pressure of 960 Pa and the atmospheric pressure of 10^5 Pa. The validation of the thermal model is based on comparing the rise time of simulated and experimental points 1 and 2 of the probe. A thermal probe which consists of 0.8 µm tungsten junction of K type micro thermocouple has been fabricated It should examine the nature of the experimental temperature sensor based on the behavior of the entire measuring chain. This particular problem will, in addition to a better definition of experimental flux densities, an important part of further work to be carried out on the subject. However, the model seems already relatively accurate because the average temperatures are closed to the experimental temperatures. The experimental rise time (average temperatures at points 1 and 2) presents the same values as atmospheric pressure, ie 25 ns. We have deliberately failed to consider a simulated average temperature over the entire head of tungsten, which has the major disadvantage of presenting a very large temperature gradient that would not ultimately more representative of the average temperature experiments.

References

[1] J.C. Godefroy, C. Gageant, D. Francis, M. Portat, "Thin film temperature sensors deposited by radio frequency cathodic sputtering", Journal of Vacuum Science and Technology A, Vol. 5, pp 2917-2923, 1987.

[2] K.G. Kreider "Thin-film transparent thermocouples", Sensors and Actuators A, Vol. 34 N°2, pp. 95-99, 1992.

[3] K.G. Kreider "Platinum/Palladium thin film thermocouples for temperature measurements on silicon wafers", Sensors and Actuators A, Vol. 69, pp. 46-52, 1998.

[4] T.H. Hoon Kim, S.J. Kim "Development of a microthermal flow sensor with thin-film thermocouples", Journal of Micromechanical and Microengineering, Vol. 16 N°11,2006.

[5] A.W. Van Herwaarden, P.M. Sarro "Thermal sensors based on Seebeck effect", Sensors and Actuators A, Vol. 10, pp. 321-346, 1986.

[6] W. Elenbass, Dissipation calorifique par convection libre sur la surface interne de tubes verticaux. Journées de la transmission de la chaleur, IFCE-Paris, pp. 379-384, 1961

[7] J. Taine, J.P. Petit, Transferts thermiques, Introduction aux sciences des transferts, 3ème édition. Edition DUNOD. Mars, 2003.

[8] Mc Adams W.H., Transmission de la chaleur, Ed. Dunod, 1961.

[9] Y. Doghman, S. Amrane, E. Gavignet, F. Lanzetta, "Dynamic characterization of a surface microthermocouple for non stationary temperature measurement", International Congress of Metrology, Paris, June 22-25, 2009.

[10] J.P. Prenel, F. Lanzetta, B. Serio, E. Gavignet, Y. Bailly, P. Nika, L. Thiery "Thermal sensor : Applications to temperature and fluidic measurements", Encyclopedia of sensors, Vol. 10, pp. 217-245, 2006.

[11] Y. Heichal, S. Chandra, E. Bordatchev, "A fast-response thin film thermocouple to measure rapid surface temperature changes", Experimental Thermal and Fluid Science, Vol. 30, pp 153-159, 2005.

[12] H. Choi, X. Li, "Fabrication and application of micro thin film thermocouples for transient temperature measurement in nanosecond pulsed laser micromachining of Nickel", Sensors and Actuators A, Vol. 136, pp. 118–124, 2007.

[13] F.E. Kennedy, D. Fruescu, J. Li, "Thin film thermocouple arrays for sliding surface temperature measurement", Wear, pp. 46-54, 1997.

[14] T.M. Berlicki, E. Murawski, M. Muszynski, S.J. Osagnik, E.L. Prociow, "Thin film thermocouples of Ge doped with Au and B", Sensors and Actuators A, Vol. 50, pp. 183-186, 1995.

[15] B. Revaz, R. Flukiger, J. Carron and M. Rappaz, "A device for measurements of the temperature response to single discharges with high local resolution and fast response time", Sensors and Actuators A, Vol. 118, pp. 238–243, 2005.

Acknowledgment

This research is issued from the French National Project SIMBA. It is supported by the French state (contract number 072906524) and the local public authorities: Région Franche-Comté & CAPM.